Wind and Structures, Vol. 2, No. 2 (1999) 105-117
DOI: http://dx.doi.org/10.12989/was.1999.2.2.105

Simulation of wind process by spectral representation method and application to cooling tower shell

Chang-Koon Choi† and Hyuk-Chun Noh‡

Department of Civil Engineering, Korea Advanced Institute of Science and Technology, Taejon 305-701, Korea

Abstract. The various spectral density functions of wind are applied in the wind process simulation by the spectral representation method. In view of the spectral density functions, the characteristics of the simulated processes are compared. The ensemble spectral density functions constructed from the simulated sample processes are revealed to have the similarity not only in global shape but also in the maximum values with the target spectral density functions with a high accuracy. For the correlation structure to be satisfied in the circumferential direction on the cooling tower shell, a new formula is suggested based on the mathematical expression representing the circumferential distribution of the wind pressure on the cooling tower shell. The simulated wind processes are applied in the dynamic analysis of cooling tower shell in the time domain and the fluctuating stochastic behavior of the cooling tower shell is investigated.

Key words: simulation; spectral density function; spectral representation; cooling tower shell.

1. Introduction

The stochasticity is a natural phenomenon typically appears in the various systems in engineering and it is very natural to assume that all the parameters in the engineering system contain intrinsically randomness to a certain extent. In the specific division of structural engineering, the spatial stochasticity appears in the material parameters and the geometrical shape of the structures (Choi 1996a, 1996b, 1998, Jullien 1994). In case of the applied loads, the stochasticity is given in mainly the time domain. The load in the random vibration theory can be seen as the white noise random process, and the earthquake load is one of the nonstationary stochastic processes. One of the most important loads in the structural systems is the wind load which is exerted on the structure as a pressure load. In particular, for the large and slender structures such as cooling tower shell, wind load is one of the most important loads. Wind load can also be classified as a stochastic process having particular spectral characteristics. To use and apply the stochastic concept in the various fields in engineering, these stochastic processes must be realized in the term of representative

† Institute Chair Professor in the Department of Civil Engineering
‡ Ph. D. Student

numerical random numbers with the specific frequency characteristics of the target power spectral density (PSD) functions. To this end, various numerical procedures are suggested and developed (Samaras 1985, Shinozuka 1991, Yousun 1990).

The problems involving the stochasticity are usually treated in the realm of Monte Carlo simulation (MCS). Generally, in the MCS, the accurate and efficient stochastic field generation algorithm is the most crucial ingredient. The generated stochastic fields should satisfy the probabilistic characteristics of the target stochastic processes. In the artificial numerical generation of stochastic processes, various schemes including covariance matrix decomposition method (Yamazaki 1990), spectral representation method (Shinozuka 1991) and ARMA (auto-regressive moving average) method (Gersch 1977, Maeda 1992, Nagamura 1987, Samaras 1985, Yousun 1990) can be used. The first two methods have the feature of the batch mode of generation as compared with the recursiveness in the scheme of ARMA. In the spectral representation method, the calculation efficiency can be achieved if the Fast Fourier Transform (FFT) technique is applied (Yang 1973).

In this paper, adopting the spectral representation method as a main tool for stochastic process generation scheme, the performance of the various PSD functions for the wind processes are investigated. The functions of Karman (1948), Davenport (1961), Kaimal (1972) and Harris (1971) PSD are chosen as trial PSD functions. As a special case of application of time varying wind pressure load, a cooling tower structure is excited by the simulated wind processes and the behavior is investigated.

2. Review of wind load

The wind velocity varies along the elevation from the ground and is given as a function of time. It can be represented as the following mathematical form.

$$u_{gust}(z,t) = \bar{u}(z) + u_d(z,t) \tag{1}$$

The usual reference wind speed is chosen as the mean wind speed at the elevation 10 m above the ground, i.e., $\bar{u}_{10} = \bar{u}(10)$ observed during the specific time duration. Generally, the wind velocity is assumed to increase with the elevation z according to the logarithmic or power law up to the maximum wind speed, known as gradient speed, which is not affected by the ground roughness. The gust fraction $u_d(z, t)$, which is the time varying fluctuating term to the constant mean wind speed, is the main target of the artificial numerical simulation to complete the wind process. The spectra of gust exhibits peak value at the low value of frequencies and distributed over a broad range of frequencies (Simiu 1996). To satisfy the features in the spectra of gust, broad range of frequency components must be taken into account in the numerical generation of wind process. Once the wind process is completed, the wind pressure load can be established using the quasi-steady areodynamic theory or a special transfer function (Reed 1983).

3. Spectral representation

In this method, a cosine series is applied to generate the stochastic process as follows (Shinozuka 1991).

$$f(t) = \sqrt{2}\sum_{n=0}^{N-1} I_n \cos(\omega_n t + \Phi_n) \tag{2}$$

The Φ_n denotes the random phase angle distributed uniformly in the interval [0, 2π]. The target PSD function $S(\omega)$ is included in the amplification term I_n as

$$I_n = \sqrt{2S(\omega_n)\Delta\omega}, \qquad n = 0, 1, 2, \cdots, N-1 \tag{3}$$

$$\omega_n = n\,\Delta\omega \tag{4}$$

$$\Delta\omega = \omega_n / N \tag{5}$$

To truncate out the higher frequency part of the PSD function, the upper cut-off frequency ω_u, beyond which the spectral density is assumed to be zero or have no significant effect on the generated process, is determined according to the specific tolerance ε. Here, the tolerance ε can be determined as follows.

$$\int_o^{\omega_u} S(\omega)\,d\omega = (1-\varepsilon)\int_o^{\infty} S(\omega)\,d\omega \tag{6}$$

In this method, a simple iterative summation operation completes the generation of stochastic process which has the required spectral features of adopted PSD function $S(\omega)$. The PSD functions $S(\omega)$ used in the generation are listed in the following section. Since the PSD function represents the spectral feature of the fluctuating component of the total time process, only the term $u_d(z, t)$ in the Eq. (1) is generated.

4. PSD functions

Through the in-situ measurement, various PSD functions for the wind process are suggested. A variety of PSD functions are listed below in terms of the frequency f and circular frequency ω.

- *Spectrum by von Karman for the along-wind direction (Karman 1948)*

$$S(f) = \frac{\sigma^2}{f}\,\frac{4\hat{f}}{\{1+(8.409\,\hat{f})^2\}^{5/6}}, \qquad \hat{f} = f\,\frac{L_{ux}(z)}{\bar{u}_{10}} \tag{7}$$

$$S(\omega) = \frac{2\pi\sigma^2}{\omega}\,\frac{4\omega^*}{\{1+(8.409\omega^*)^2\}^{5/6}}, \qquad \omega^* = \frac{\omega}{2\pi}\,\frac{L_{ux}(z)}{\bar{u}_{10}}, \qquad \sigma^2 = \beta u_*^2 \tag{8}$$

- *Spectrum by Kaimal (Kaimal 1972)*

$$S(f) = \frac{u_*^2}{f}\,\frac{200\,\hat{f}}{(1+50\,\hat{f})^{5/3}}, \qquad \hat{f} = f\,\frac{z}{\bar{u}_{10}} \qquad S(\omega) = \frac{2\pi u_*^2}{\omega}\,\frac{200\,\hat{\omega}}{(1+50\,\hat{\omega})^{5/3}}, \qquad \hat{\omega} = \frac{\omega}{2\pi}\,\frac{z}{\bar{u}_{10}} \tag{9}$$

- *Spectrum by Harris (Harris 1971)*

$$S(f) = \frac{u_*^2}{f}\,\frac{4.0d}{(2+d^2)^{5/6}}, \qquad d = \frac{1800f}{\bar{u}_{10}} \qquad S(\omega) = \frac{2\pi u_*^2}{\omega}\,\frac{4d}{(2+d^2)^{5/6}}, \qquad d = \frac{900\omega}{\pi\bar{u}_{10}} \tag{10}$$

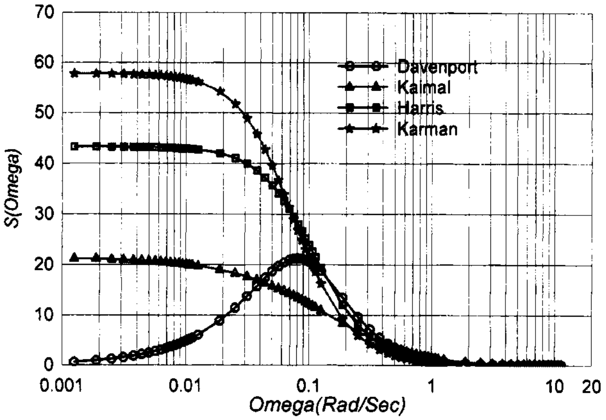

Fig. 1 Plot of PSD functions

- *Spectrum by Davenport (Davenport 1961)*

$$S(f)=\frac{u_*^2}{f}\frac{40c^2}{(1+c^2)^{4/3}},\quad c=\frac{1200f}{\bar{u}_{10}}\quad S(\omega)=\frac{2\pi u_*^2}{\omega}\frac{4\xi^2}{(1+\xi^2)^{4/3}},\quad \xi=\frac{600\omega}{\pi\bar{u}_{10}} \tag{11}$$

In the above, L_{ux} is the integral scale of turbulence which measures the average size of the turbulent eddies of the flow. The larger the L_{ux}, the smaller the root-mean-square of generated wind process. It is one of 9 components of integral scale of turbulence. The parameter β is given depending on the roughness length z_0. The mean wind velocity and the roughness length z_0 are related to each other as in the following equation, which enables the calculation of the friction velocity u_* at the elevation z.

$$u(z)=\frac{1}{\kappa}u_*\ln\frac{z}{z_o} \tag{12}$$

where, κ is the Karman constant which is approximated as 0.4. The root-mean-square of the wind velocity σ defined as given in the above (Eq. 8) in conjunction with β and u_*. The plot of PSD functions is given in Fig. 1.

5. Numerical simulation and discussions

The wind process having mean speed of 20 m/sec at the elevation of 10 m above the ground is taken as base data for the simulation of wind process. The roughness length z_o is assumed to be 0.07 m which corresponds to the value of $\beta=6.0$. The value of β decreases as the roughness length increases.

Fig. 2 shows the wind processes generated based on the spectral density functions of Karman, Kaimal, Harris and Davenport, sequentially from (a) to (d). Among the 200 generated sample processes only three of them are plotted for simplicity. As expected from the spectral content character of the PSD functions as shown in Fig. 1, the processes by the Karman and Harris spectra include a little larger effect of lower frequency components than

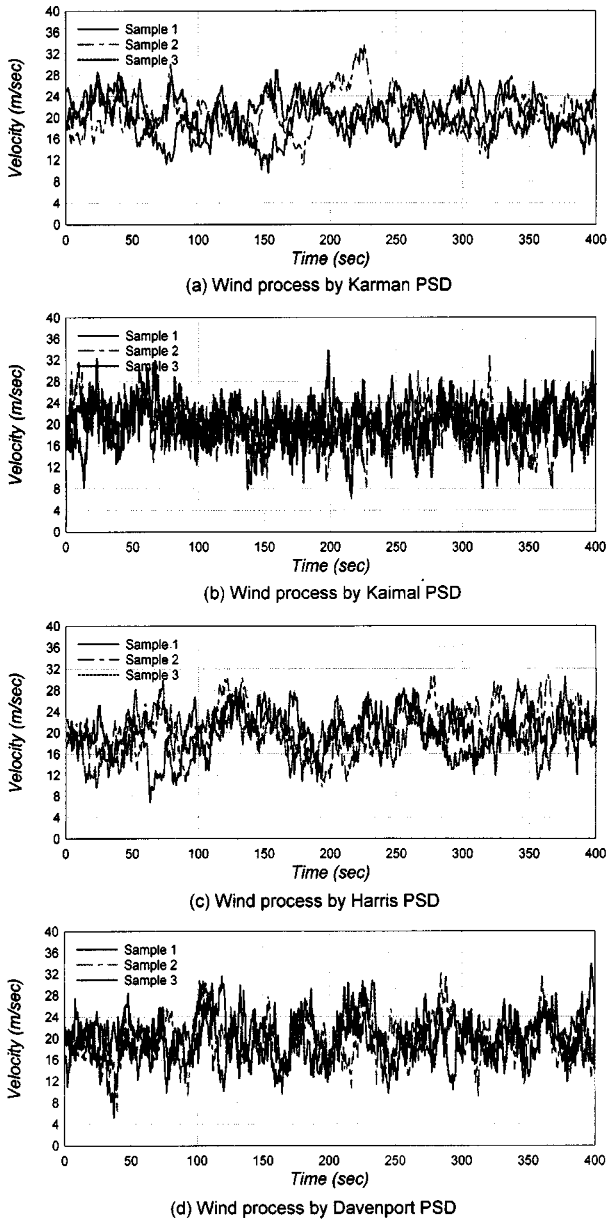

Fig. 2 Generated samples by respective PSD functions

those by the Kaimal and Davenport. In the processes by Kaimal PSD function, more higher frequency terms are included than the others. The processes simulated based on the Karman, Harris and Davenport PSD functions look similar to the records of site investigations (Simiu 1996). However, it seems like that all the simulated processes contain relatively large effects of higher frequencies when compared with those of site investigations.

In the realization of the wind processes, the following parameters are applied to satisfy the requirements of the spectral representation algorithm of Eqs. (2)-(5).

Table 1 Simulation parameters

PSD	Δt(sec)	Data number	N	ε	ω_u(rad/sec)	Area	T_o(sec)
Karman	1.00	2048(2048)	1000	0.050	3.09	8.269	2034
Kaimal	0.30	2048(614)	800	0.075	8.75	8.158	575
Harris	0.50	2048(1024)	700	0.050	4.40	9.184	999
Davenport	0.40	2048(819)	900	0.050	7.16	8.227	790

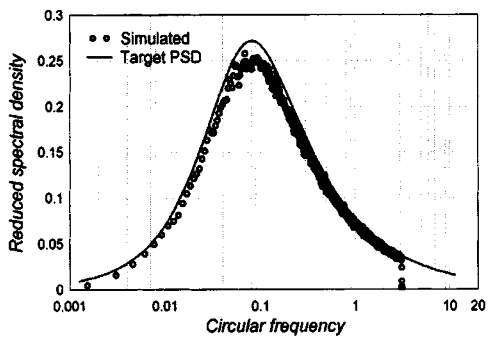

(a) PSD of Karman

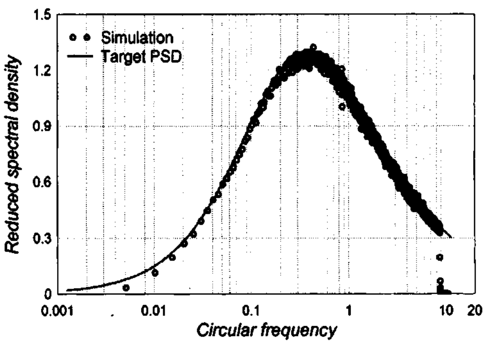

(b) PSD of Kaimal

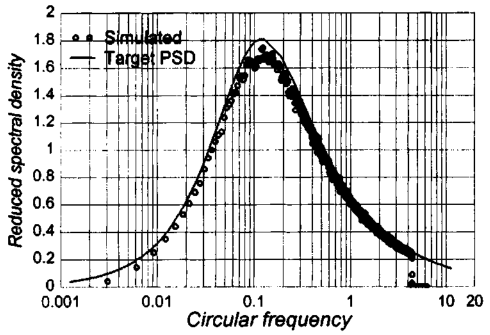

(c) PSD of Harris

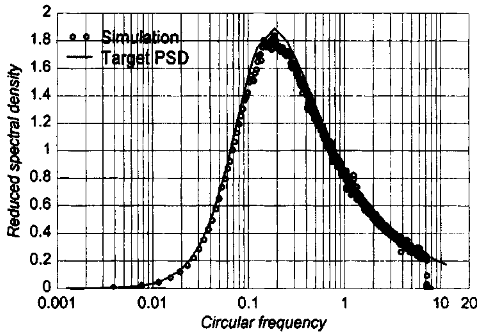

(d) PSD of Davenport

Fig. 3 Comparison of target and simulated PSD functions

The ensemble PSD functions by the simulated processes are compared with those of the target functions in Fig. 3. In all the cases, it has been observed that the similarity not only in global shape but also in the maximum values of the simulations and targets are attained with a high accuracy. As seen in the figure, the frequency region higher than the upper cut-off frequency ω_u is not included in the simulation procedures. Since the wider the range of frequencies taken into account, the higher the computational cost may result in, the sacrifice of accuracy with a tolerable limit is inevitable. Furthermore, the high frequency component has very low energy as seen in the plot of PSD (Fig, 3), which makes the omission of higher frequency as rational. With the tolerance ε in Table 1, the $(1-\varepsilon)\times 100$ percent of the total area of PSD function is actually taken into account in the simulation procedure.

In Fig. 3, the reduced spectral density is the modified PSD function as follows.

Table 2 Comparison of root-mean-square of process simulation

PSD	RMS for original k=0.4	RMS of modified k=0.1165
Karman	13.513	3.940
Kaimal	13.209	3.850
Harris	14.241	4.131
Davenport	13.564	3.940

$$\text{Reduced spectral density} = S(\omega)\frac{\omega}{\sigma^2} \tag{13}$$

The root-mean-square of the wind process is denoted as σ and given as a function of friction velocity u_* and parameter β as

$$\sigma = \sqrt{\beta u_*^2} \tag{14}$$

According to Eq. (12), the friction velocity u_* is written as

$$u_* = \frac{u(z)\,\kappa}{\ln\dfrac{z}{z_o}} \tag{15}$$

Therefore, if the simulation parameters are substituted into the above two Eqs. (14) and (15), the root-mean-square of wind speed is obtained as 3.949 m/sec ($u(z)$=20 m/sec, $\kappa\approx0.4$, β=6.0, z_o=0.07, z=10.0 m). However, if the Karman constant κ is used as given in the literature (Simiu 1996), the root-mean-square of wind velocity in the simulation is obtained to be greater than that of the theoretical one given by Eq. (14). If the Karman constant κ in Eq. (15) is modified approximately as 0.1165, the obtained root-mean-square of simulated wind velocity is observed to be similar to that of theory. Table 2 shows the root-mean-square results of the simulated wind processes in case of the original and modified Karman constant.

6. Example of application

In applying the wind load to the structural analysis, some prerequisite requirements must be satisfied by the generated wind processes. The time varying character of wind implies that the wind process possesses some features to be satisfied in time domain. These features are presented in the PSD function which defines the time dependent wind behaviors in the frequency domain. One of the other requirements is related to the structure itself. Since the wind velocity is a function of elevation from the ground and is dependent on the location on the structure, the spatial correlation must be satisfied between two distinct points on the structure. The wind load on the cooling tower shell should be one example of a special case.

In case of cooling tower shells, wind tunnel test gives good experimental results for the correlation structures on the surface of the shell (Kasperski 1988), and a good mathematical approximation for the correlation structure is suggested by Zahlten (1998) relying only on the eye-investigation of the experimental correlation structure. In this study, however, it is noted

Table 3 Fourier coefficients used in representation of covariance matrix

Coefficient C_n	Value	Coefficient C_n	Value
C_0	-0.11670	C_7	-0.04474
C_1	-0.27918	C_8	-0.00833
C_2	-0.61978	C_9	-0.00973
C_3	-0.50927	C_{10}	-0.01356
C_4	-0.09167	C_{11}	-0.00597
C_5	0.11794	C_{12}	-0.01667
C_6	0.03333		

that the correlation structure resulted from the wind tunnel test has almost similar distribution of the wind pressure along the circumferential direction obtained by the wind tunnel test. Therefore, based on the mathematical expression of the wind pressure along the circumference of cooling tower shell, a different type of mathematical expression to represent the correlation structure is given as follows.

$$\rho_{ij}^{w}(\theta_i, \theta_j) = \frac{e^{-\lambda r_1}\left(\sum_{n=0}^{12} C_n \cos n r_1\right) + e^{-\lambda r_2}\left(\sum_{n=0}^{12} C_n \cos n r_2\right)}{(1+e^{-2\pi\lambda})\sum_{n=0}^{12} C_n} \tag{16}$$

where

$$r_1 = |\theta_i - \theta_j|, r_2 = -r_1 + 2\pi \tag{17}$$

The C_n's are the Fourier coefficients used to represent the circumferential distribution of the wind pressure, and are given in Table 3. The results obtained by the value of λ=1.2 in Eq. (16) is similar to the experimental correlation matrix and therefore λ=1.2 is considered to be suitable for the practical use.

The correlation matrices along the circumferential direction given by Zahlten (1998) with the corrected parameter λ_e=1.445 (0.445 as given in their paper seems to be a typographical error) and the one suggested in this study are given in Fig. 4 for comparison. The two correlation structures are similar to each other in the global trend. However, the proposed correlation structure has theoretical base in formulation because it is deduced from the formula representing the circumferential wind pressure distribution on the surface of the cooling tower shell as given in the following equation.

$$p(z, \theta) = \frac{1}{2}\rho_a v_{10}^2 \left(\frac{z}{10}\right)^{\frac{2}{7}} \cdot \sum_{n=0}^{12} C_n \cos n\theta \tag{18}$$

The power spectral density function of the proposed correlation matrix in Eq. (16) can be obtained by the inverse Fourier transform of the correlation matrix. The resulting function takes the following expression.

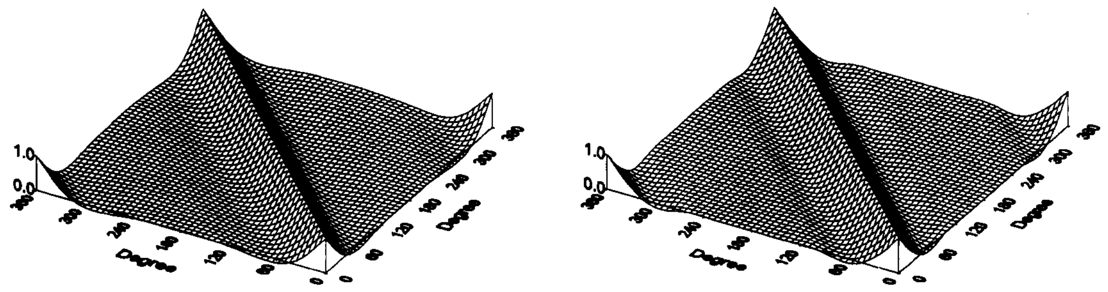

(a) Correlation matrix (Zahlten 1998) (λ_e =1.445) (b) Proposed Fictive correlation matrix (λ =1.2)

Fig. 4 Comparison of correlation matrices

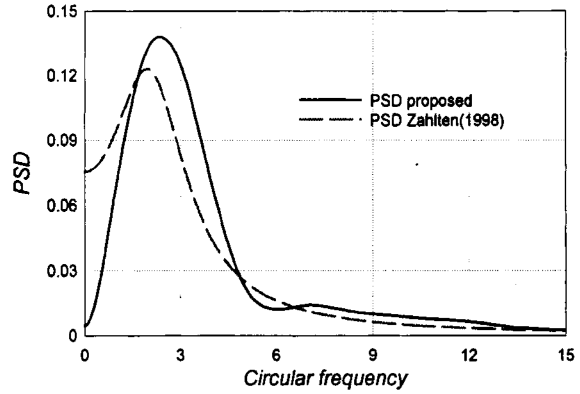

Fig. 5 Comparison of PSD functions

$$S(\omega) = \frac{\lambda}{2\pi} \frac{1-e^{-2\pi\lambda}}{1+e^{-2\pi\lambda}\sum_{n=0}^{12} C_n} \sum_{n=0}^{12} C_n \left\{ \frac{1}{\lambda^2+(-n+|\omega|)^2} + \frac{1}{\lambda^2+(n+|\omega|)^2} \right\} \tag{19}$$

The PSD functions suggested by Zahlten (1998) and in this study are compared in Fig. 5.

The constructed correlation structure of the wind processes by the PSD in Eq. (19) is shown in Fig. 6, which is very similar to that of the mathematical one (Fig. 4).

To apply the time series of wind load to the cooling tower shell, independent time processes can be generated with respect to the two positioning variables z and θ in the meridional and circumferential directions. Fig. 7b shows the position dependent wind pressure processes at the indicated data points (Fig. 7a) on the cooling tower shell.

Since only the wind history is scaled with the pressure coefficient, the turbulence intensity of the wind pressure takes almost same values independent of the position along the circumference of cooling tower shell (Fig. 7b). The positive and negative pressures imply the pressure onto the shell and suction force out of the shell, respectively. The circumferential distribution and the data points of the wind pressure history are shown in Fig. 7(a). The wind pressure distribution in Fig. 7(a) is the one which includes the effect of the internal suction, which resulted in the pushing pressure in the rear part of the shell.

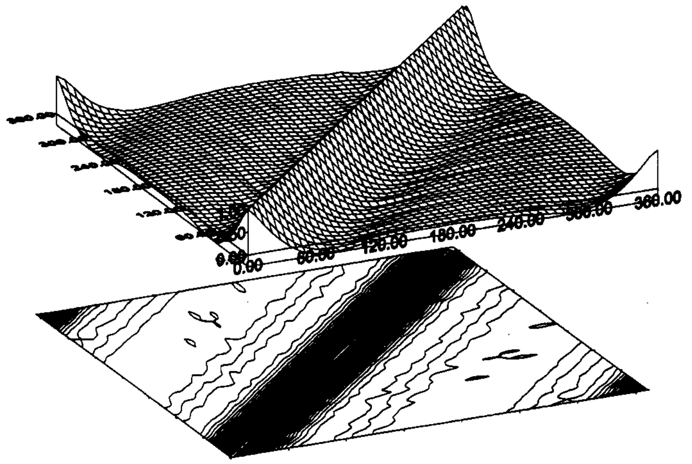

Fig. 6 Generated correlation matrix

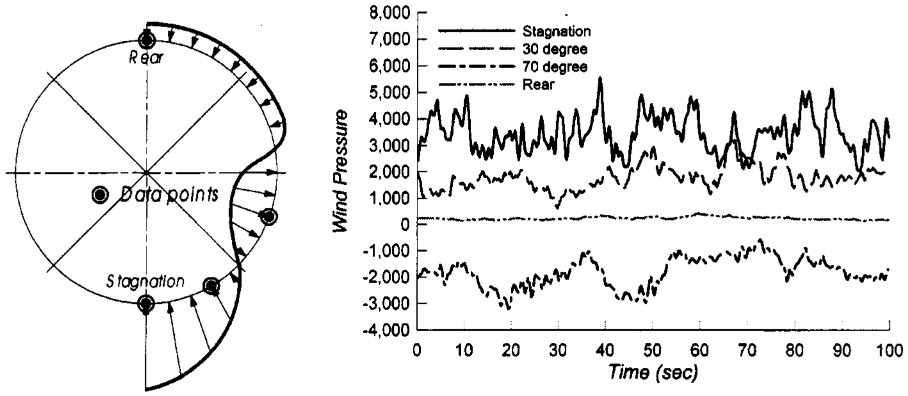

(a) Cross section (b) Wind pressure history

Fig. 7 Fluctuating wind pressure along the circumference

The Port Gibson cooling tower at Mississippi having total height of 159.6 m is taken as an example structure. This cooling tower has 9.1 m(30ft) long base support columns. The Port Gibson tower is excited by the simulated moderate and severe wind conditions. The moderate wind means the wind process which has the turbulence intensity of 0.2 (when κ=0.1165). The turbulence intensity is 0.7 in case of the severe wind condition (when κ=0.4). The mean wind velocity is assumed to be 29.16 m/sec. In this case the static displacement at the throat is obtained as 3.41 cm. The displacement histories at the throat level are given in Fig. 8. To avoid the impact effect of the suddenly applied wind load, which is not the real case, the applied load factor is increased from zero to 1.0 for the first 5 seconds. After then the steady gusty wind pressure starts to be applied. The analysis in the first 5 seconds is a kind of pre-analysis, therefore if the response statistics are required, the time history of response in this interval is excluded.

The response of structure exhibits fluctuating phenomenon showing the effects of stochastic pressure load and of the dynamic resonance. Since the simulated wind processes are the

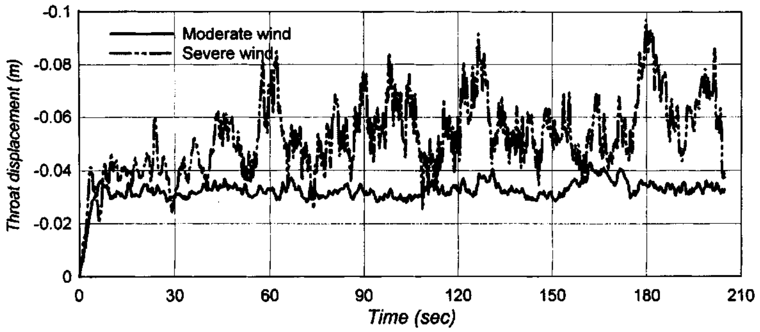

Fig. 8 Example analysis of cooling tower shell

stationary Gaussian processes, the temporal statistics can give the statistics of the response. Therefore, if the extended full scale analysis is performed, the root-mean-square of the response due to the stochastic pressure load can be found and the more precise investigation on the behavior of cooling tower system can be expected.

7. Conclusions

The simulation of wind processes based on the various power spectral density functions proposed by Karman, Kaimal, Harris and Davenport is performed using the spectral representation method. To verify whether the simulated processes satisfy the requirement of the PSD functions, the ensemble PSD functions are constructed from the simulated processes by the Fast Fourier transform. The simulated and target PSD functions are in good agreement with each other. Through the comparison of the simulated processes, it is noted that the processes simulated by Karman, Harris and Davenport PSD functions are more similar to that of the field investigated histories than that of the PSD of Harris, where the wind processes including higher frequencies are obtained. To construct the correlation structure in the circumferential direction, a new mathematical expression based on the formula representing the circumferential distribution of the wind pressure is suggested.

The simulated wind pressure load is applied to the example analysis of the cooling tower shell to investigate the dynamic behavior in time domain. The wind load is distributed in the similar way as the distribution of the pressure coefficient in the circumferential direction, which is consistent with the distribution of the wind pressure on the cooling tower shell. As the time dependent fluctuating time history of the cooling tower shell is obtained in the example analysis, if the extended full scale analysis is performed, the more precise investigation on the behavior of cooling tower system can be expected. Since the resonance phenomenon can also be observed, it will be helpful to obtain the dynamic amplification factor in a more precise way.

Acknowledgements

This work was partially supported by the Korea-Germany cooperative science program under the auspices of the Korea Science and Engineering Foundation (KOSEF).

References

Bartoli, G., Borri, C. and Zahlten, W. (1992), "Nonlinear dynamic analysis of cooling tower under stochastic loading", *Journal of Wind Engineering and Industrial Aerodynamics*, 41-44.

Choi, C.K. and Noh, H.C. (1996a), "Analysis of geometrically imperfect cooling tower shell considering the effect of tension stiffening of concrete", *Proceedings of the 4th International Symposium on Natural Draught Cooling Towers*, Eds. By U.Wittek and W.B. Kratzig, 141-149.

Choi, C.K. and Noh, H.C. (1996b). "Nonlinear analysis of cooling tower shells with cyclic shape imperfections", *APCOM'96*, **2**, 1437-1443, Seoul, Korea, August 16-18.

Choi, C.K. and Noh, H.C. (1998), "The stochastic analysis of the shape imperfection of cooling tower shells", *SEWC(Structural Engineers World Congress)*, In CD-ROM, San Francisco, California, USA. July 18-23.

Davenport, A.G. (1961), "The spectrum of horizontal gustiness near the ground in high winds", *J. Royal Meteorol. Soc.*, **87**, 194-211.

Gersch, W. and Yonemoto, J. (1977), "Synthesis of multivariate random vibration system : a two-stage least squares AR-MA model approach", *Journal of Sound and Vibration*, **52**(4), 553-565.

Harris (1971), "The nature of wind", in The Modern Design of Wind-Sensitive Structures, Construction Industry and Information Association, London, U.K.

Jullien, J.F., Aflak, W. and L'Huby, Y. (1994). "Cause of deformed shapes in cooling towers", *J. Struct. Engrg., ASCE*, **120**(5), May, 1471-1488.

Kaimal, J.C. *et al.* (1972), "Spectral characteristics of surface-layer turbulence", *J. Royal Met. Soc.*, **98**, 563-589.

Kapania, R.K. and Yang, T.Y. (1984), "Time domain random wind response of cooling tower", *Journal of Engineering Mechanics, ASCE*, **110**(4), 1524-1543.

Kasperski, M. (1988), "Identification of design-relevant load portions from stochastic processes exemplified for natural draught cooling towers under wind loading", Technical Report 88-6, Department of Civil engineering, University of Bochum.

Maeda, J. and Makino, M. (1992), "Characteristics of gusty winds simulated by an ARMA model", *Journal of Wind Engineering and Industrial Aerodynamics*, **41-44**.

Mignolet, M.P. and Spanos, P.D. (1990), "MA to ARMA modeling of Wind", *Journal of Wind Engineering and Industrial Aerodynamics*, **36**, 429-438.

Nagamura, T., Deodatis, G. and Shinozuka, M. (1987), "ARMA model for two-dimensional processes", *Journal of Engineering Mechanics, ASCE*, **113**(3), 234-251.

Niemann, H, -J. (1984), "Modeling of wind loads with regard to gust effects", *Engineering Structures*, **6**, Oct. 274-280.

Reed, D.A. and Scanlan, Robert H. (1983), "Time series analysis of cooling tower wind loading", *Journal of Structural Engineering, ASCE*, **109**(2), 538-554.

Samaras, E., Shinozuka, M. and Tsurui, A. (1985), "ARMA representation of random processes", *Journal of Engineering Mechanics, ASCE*, **111**(3), 449-461.

Shinozuka, M. and Deodatis, G. (1991), "Simulation of stochastic processes by spectral representation", *ASME, Applied Mech. Rev.* **44**(4), April, 191-203.

Simiu, E. (1979), "Laboratory simulation of turbulent wind spectra", *Engineering Mechanics Division*, **105**(EM6), 1050-1054.

Simiu, E. and Scanlan, R.H. (1996), "Wind effects on structures, fundamentals and applications to design", The Third Edition, John-Wiely & Son, Inc.

Sun, T. F., Gu, Z. F., Zhou, L. M., Li, P. H. and Cai, G. L. (1992), "Full-scale measurement and wind-tunnel testing of wind loading on two neighboring cooling towers", *Journal of Wind Engineering and Industrial Aerodynamics*, **41-44**, 2213-2224.

von Karman, T. (1948), "Progress in the statistical theory of turbulence", *Proc. Nat. Acad. Sci.*, Washington, D.C, 530-539.

Yamazaki, F. and Shinozuka, M. (1990), "Simulation of stochastic fields by statistical preconditioning", *Journal of Engineering Mechanics, ASCE*, **116**(2), 268-287.

Yang, J.-N. (1973), "On the normality and accuracy of simulated random process", *Journal of Sound and Vibration,* **25**(1), 73-85.
Yousun Li and Kareem, A. (1990), "ARMA representation of wind filed", *Journal of Wind Engineering and Industrial Aerodynamics,* **36**, 415-427.
Zahlten, W. and Borri, C. (1998), "Time-domain simulation of the non-linear response of cooling tower shells subjected to stochastic wind loading", *Engineering Structures,* **20**(10), 881-889.

(Communicated by Managing Editor)